Bull. Chem. Soc. Ethiop. **2024**, 38(1), 147-166.
DOI: https://dx.doi.org/10.4314/bcse.v38i1.12

ISSN 1011-3924
Printed in Ethiopia
Online ISSN 1726-801X

NEW IRON(III), COBALT(II), NICKEL(II), COPPER(II), ZINC(II) MIXED-LIGAND COMPLEXES: SYNTHESIS, STRUCTURAL, DFT, MOLECULAR DOCKING AND ANTIMICROBIAL ANALYSIS

Hany M. Abd El-Lateef[1,2*], Ali M. Ali[2], Mai M. Khalaf[1,2*] and Aly Abdou[2]

[1]Department of Chemistry, College of Science, King Faisal University, Al-Ahsa 31982, Saudi Arabia
[2]Department of Chemistry, Faculty of Science, Sohag University, Sohag 82534, Egypt

(Received October 11, 2023; Revised November 8, 2023; Accepted November 9, 2023)

ABSTRACT. The present framework has as its goal the design and synthesis and characterization of new mononuclear 1:1:1 (M:L:Q) mixed-ligand complexes, including FeLQ, CoLQ, NiLQ, CuLQ, and ZnLQ. The "L," is the 4-[(4-oxo-4,5-dihydro-1,3-thiazol-2-yl)hydrazono]methylphenyl 4-methylbenzenesulfonate, while the "Q," is the 8-hydroxy quinoline. According to the findings, L and Q ligands each play the role of a neutral bi-dentate NN and a monobasic bi-dentate ON ligand, respectively. The findings demonstrated an octahedral shape. The density functional theory (DFT) technique was employed, and the quantum chemical descriptors were assessed, to optimize the molecular structure of the compounds. An *in vitro* investigation was carried out to investigate the antibacterial and antifungal activities of the compounds. According to the findings, the activity of metal complexes as potential candidates for use as antibiotics and antifungals is much greater than that of their free ligands. The in-silico inhibition of the 1fj4 protein was investigated using molecular docking. ZnLQ complex was the one that inhibited the 1fj4 protein with the greatest degree of success. The fact that this is the case lends credence to the notion that these compounds have the potential to function as launchpads for the development of new classes of antibiotics.

KEY WORDS: Metal complexes, Schiff-base, Antimicrobial, DFT, Molecular docking

INTRODUCTION

More and more data suggests that transition metal ions play an important role in several essential biological processes [1]. Due to the fact that the action of a great number of medications is reliant on the coordination with metal ions or the suppression of the development of metalloenzyme [2]. The properties of metals, which may have a broad range of coordination numbers, geometries, and varying oxidation states, and the capacity to bind a variety of organic ligands or mixed ligands are combined in coordination compounds [3]. It has been discovered that a number of different antibiotics have a metal-binding site, and there have been several studies published on the subject of complex metals and their functions in biological activities [4]. Effective antibiotic action may sometimes be attributed to the presence of transition metal ions that are bonded in stable coordination linkages that play an essential part in the structure of the antibiotic. Complexes often display better physicochemical properties and are substantially more powerful than their parent drugs [5]. The effective operation of some antibiotics requires the presence of metal ion cofactors. The metalloenzymes and other biological processes rely heavily on the coordination chemistry of mixed ligands with transition and non-transition metal ions [6]. In the vast majority of cases, metal complexes have a greater level of bioactivity than free ligands [7]. In addition, complexation may reduce the severity of certain adverse effects and medication resistance. Mixed ligand complexes are distinguished from other forms of complexes by the presence of at least two distinct ligand classes covalently linked to the same metal ion. When a complex contains more than one kind of ligand, it is more probable than not that the complex will exhibit characteristics that are distinct

*Corresponding author. E-mail: hmahmed@kfu.edu.sa, hany_shubra@science.sohag.edu.eg (Hany M. Abd El-Lateef.); aly_abdou@science.sohag.edu.eg, aly_abdou@yahoo.com (Aly Abdou)

from those expected for the complex. As a result of this, researchers are interested in creating mixed ligand groups that have a variety of properties [8, 9].

Biological activities of metal complexes are influenced by various factors, such as the type of metal ion, the nature and number of ligands, the geometry and stability of the complex, and the interaction with biological molecules and systems. Herein, we will discuss some of the biological activities derived from iron(III), cobalt(II), nickel(II), copper(II), zinc(II) mixed-ligand complexes based on 4-[(4-oxo-4,5-dihydro-1,3-thiazol-2-yl)hydrazono]methylphenyl 4-methyl-benzenesulfonate (L1), and 8-hydroxy quinoline (L2) [10-16].

L1 is a thiosemicarbazone derivative that has been reported to have antibacterial, antifungal, antiviral, anticancer, and anti-inflammatory properties [17-23]. L2 is a well-known chelating agent that can form stable complexes with various metal ions and has been shown to have antimicrobial, antitumor, antioxidant, and neuroprotective effects. The combination of L1 and L2 as mixed-ligands can enhance the biological activities of the metal complexes by increasing their solubility, stability, and selectivity.

Some of the biological activities derived from the mixed-ligand complexes are [10-16]: Antimicrobial activity: The mixed-ligand complexes have been tested against different strains of bacteria and fungi and have shown significant inhibitory effects. The complexes exhibit higher antimicrobial activity than the free ligands or the metal salts alone. The antimicrobial activity of the complexes depends on the type of metal ion, the ratio of the ligands, and the structure of the complex. The complexes can interact with the cell membrane or wall of the microorganisms and disrupt their functions or cause cell lysis. Antioxidant activity: The mixed-ligand complexes have been evaluated for their ability to scavenge free radicals and protect biomolecules from oxidative damage. The complexes show higher antioxidant activity than the free ligands or the metal salts alone. The antioxidant activity of the complexes depends on the type of metal ion, the ratio of the ligands, and the redox potential of the complex. The complexes can donate electrons or hydrogen atoms to neutralize free radicals or chelate metal ions that catalyze oxidative reactions. Anticancer activity: The mixed-ligand complexes have been screened for their cytotoxicity against different types of cancer cells and have shown promising results. The complexes exhibit higher anticancer activity than the free ligands or the metal salts alone. The anticancer activity of the complexes depends on the type of metal ion, the ratio of the ligands, and the mode of action of the complex. The complexes can induce apoptosis or necrosis in cancer cells by interfering with their DNA synthesis or repair, mitochondrial function, or cell cycle regulation.

In conclusion, iron(III), cobalt(II), nickel(II), copper(II), and zinc(II) mixed-ligand complexes based on L1 and L2 have various biological activities that can be exploited for therapeutic purposes. The mixed-ligand approach can improve the biological activities of the metal complexes by modulating their physicochemical properties and biological interactions.

In this article, a fresh collection of 1:1:1 metal:ligand:co-ligand complexes will be synthesized and investigated. The 1fj4 protein will be used for testing not only the in vitro antibacterial and antifungal efficacy of new drugs but also its molecular docking capabilities. Testing will also be done in vitro to establish whether or not the new medicines are able to suppress the activity of 1fj4. In addition, a density functional theory (DFT) investigation was carried out in order to look at the atomic characteristics of the molecule as well as its structure.

EXPERIMENTAL

Synthesis

Preparation of the L ligand

The ligand (L) was synthesized by treating the molecule 4-[(carbamothioylhydrazono) methyl] phenyl 4-methylbenzenesulfonate with ethyl bromoacetate, which led to the formation of the

corresponding ethyl 4-[(4-oxo-4,5-dihydro-1,3-thiazol-2-yl)hydrazono] methyl-phenyl 4-methyl, Scheme (1).

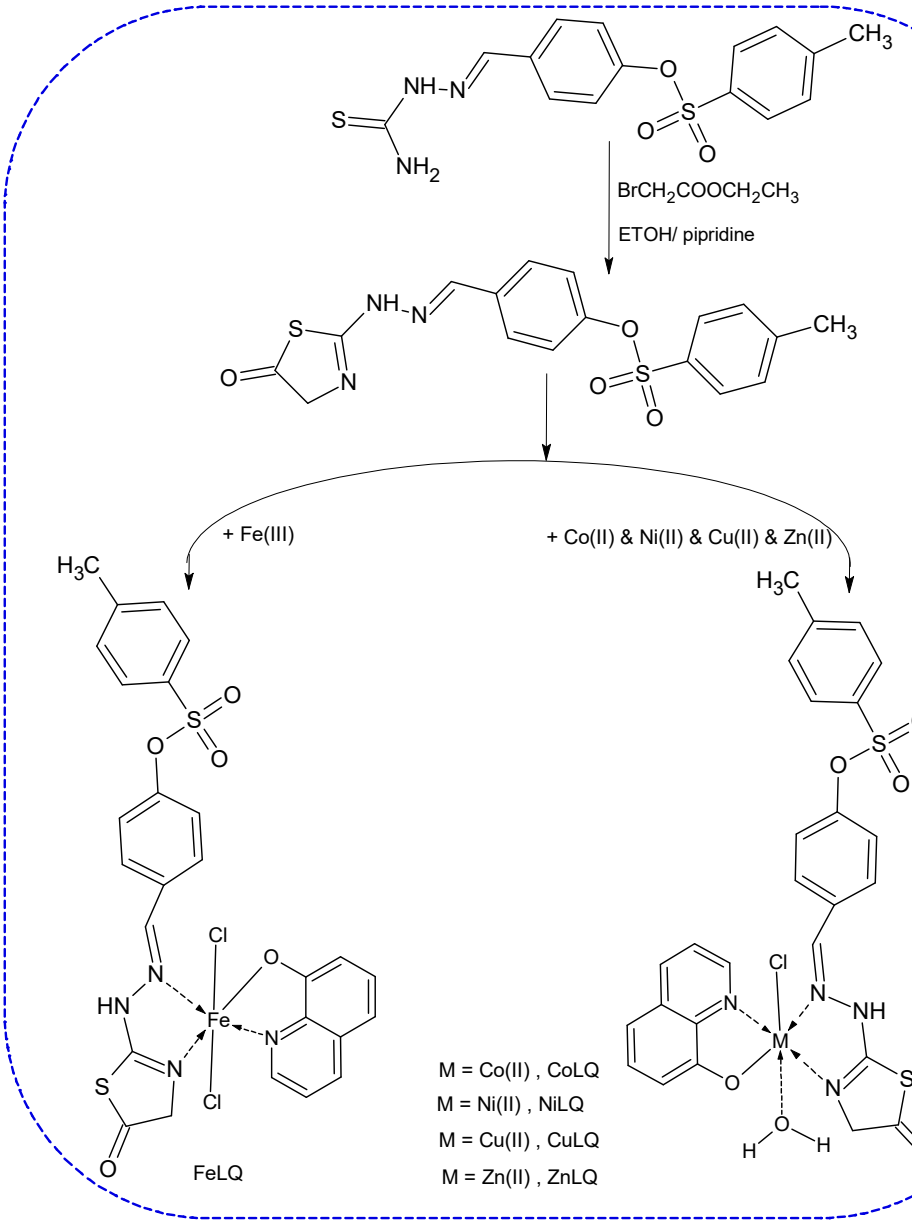

Scheme 1. Synthesis of the ligand (L) and its metal complexes.

Synthesis of the mixed-ligand complexes

In order to generate metal complexes in a ratio of (M:L:Q 1:1:1 molar ratio) [24], it was necessary to mix together equal volumes of Schiff-base (L) and 8-hydroxy quinoline (HQ) solutions in hot ethanol, along with 15 mL of an aqueous solution made from the metal salt. The combination was kept in a water bath at a temperature of 80 ºC for a period of 12 h, during which time it was allowed to reflux. The temperature of the water bath was kept at the same level throughout the experiment. After that, the finished product underwent many rounds of filtration and washing in a solution consisting of water and ethanol at a ratio of 1:4 water to ethanol. The precipitated complexes were put on anhydrous calcium chloride and allowed to dry in desiccators before being re-crystallized from a solution of water and ethanol (1:4), as shown in Scheme 1. This step was necessary before the complexes could be re-crystallized.

3D-Molecular modeling

Combining the hybrid correlation functional (B3LYP) and the LANL2DZ and 6-311 (d,p) basis sets allowed for the Optimization of the geometry of the necessary materials. This process was carried out employing the relevant materials. This technique was applied to both ligand complexes and metal complexes. In order to analyze quantum chemical characteristics, we made use of both the LUMO and HOMO energies. These qualities include, but are not limited to, electron affinity (EA), ionization potential (IP), electronegativity (χ), gap energy (ΔE), chemical hardness (η), softness (σ), chemical potential (CP), maximum electronic charge (N_{max}), electrophilicity index (ω), and nucleophilicity index (Nu) [25, 26].

Antimicrobial in vitro testing

Aspergillus flavus, *Trichophyton rubrum*, and *Candida albicans* were the three fungus strains that were used in the in vitro antibacterial assessment of the free ligands and their mixed-ligand complexes. In addition, two gram-positive bacterial strains, namely *S. aureus* (G+) and *B. cereus* (G+), as well as two gram-negative bacterial strains, namely *P. aeruginosa* (G-) and *E. coli* (G-), were used. In experiments [27], the well disc diffusion technique was applied.

The antibacterial and antifungal activity of the conventional antibiotic chloramphenicol was identified under the same circumstances, and the results were compared to those of the compounds that were under investigation. The following equation [28] was used in order to calculate the activity index, which was expressed as a percentage:

$$\mathrm{AI}/\% = \left(\frac{\mathrm{IZ}^{\mathrm{t}}}{\mathrm{IZ}^{\mathrm{s}}}\right) \times 100 \qquad (1)$$

where IZ^{t} and IZ^{s} are the inhibition zone by the test and the standard compounds, respectively.

Molecular docking examination

We utilized molecular docking to determine whether or not the compounds in question had the potential to bind to *E. coli* (the structure of beta-ketoacyl-[acyl carrier protein] synthase in association with thiolactomycin, implications for drug design, PDB ID: 1FJ4) [29]. This allowed us to determine both the therapeutic efficacy of the compounds in issue and whether or not they might potentially bind to *E. coli* [30]. Because of this, we were able to determine whether or not the chemicals found in this problem had the potential to bind to *E. coli*.

RESULTS AND DISCUSSION

Confirmation of the mixed-ligand complexes' structure

Molar conductance and elemental analysis

Acetone, dimethylformamide, and dimethyl sulfoxide were the only solvents that were successful in dissolving the isolated complexes. The fact that the findings of the microanalysis for the carbon, nitrogen, and hydrogen of the metal complexes demonstrated that there was a good match between the estimated and discovered values lends credence to the suggested formula, which can be seen in Table 1. The fact that the complexes had low values for their molar conductivity demonstrated that the complexes were not electrolytes [31], as shown in Table 1.

Binding mode and FT-IR spectrum

The FT-IR spectrum data provided conclusive evidence on the manner of ligand binding with metal ions [32]. In order to establish the coordination sites that may be involved in chelation, IR spectra of metal complexes were compared with those of free ligands. The results of this comparison are shown in Table 1.

Table 1. Physical properties, elemental analysis: found (calc.) %, conductivity (μ_v, $\Omega^{-1}cm^2mol^{-1}$), FT-IR, UV-vis., magnetic, and stoichiometry of the prepared compounds.

Parameter		HQ	L	FeLQ	CoLQ	NiLQ	CuLQ	ZnLQ
Physical properties	Color	White	Yellow	Dark yellow	Deep orange	Red-orange	Pale blue	Yellow
	Yield (%)	--	90	85	88	94	90	89
	m.p. (ºC)	77	82	278	289	280	288	258
Elemental analysis Found (calc.) %	C	--	52.43 (52.08)	47.55 (47.29)	48.13 (48.34)	48.68 (48.36)	48.41 (48.00)	47.38 (47.86)
	H	--	3.88 (4.15)	3.45 (3.21)	3.87 (3.59)	3.31 (3.59)	3.27 (3.56)	3.25 (3.55)
	N	--	10.79 (10.18)	8.78 (8.48)	8.27 (8.67)	8.28 (8.68)	8.34 (8.61)	8.82 (8.59)
	M	--	--	8.77 (8.46)	9.01 (9.12)	9.45 (9.09)	9.42 (9.77)	10.28 (10.02)
Conductivity	μ_v, $\Omega^{-1}cm^2mol^{-1}$	--	--	10.27	11.24	10.75	10.19	9.88
FT-IR spectra	υ (-OH)$_{HQ}$	3370	--	3450	3465	3469	3478	3480
	υ (-C=N)$_{HQ}$	1588	--	1534	1538	1532	1530	1538
	υ (-CH=N)	--	1652	1594	1590	1589	1597	1588
	υ(C=N) thiazole	--	1597	1570	1568	1566	1573	1570
	υ (M-O)	--	--	530	524	527	533	531
	υ (M-N)	--	--	445	440	438	440	442
UV-Visible	λ_{max} (nm)	260,350	240, 315	385	475	540	550	400
Magnetic	μ_{eff} (B.M)	--	--	5.94	4.85	3.17	1.93	Dia
Stoichiometry	M : L	--	--	1:1:1	1:1:1	1:1:1	1:1:1	1:1:1

The azomethine group (-CH=N) stretching vibration (1652 cm^{-1}) was moved to lower wave numbers following coordination for the Schiff-base ligand (L), as shown in Table 1. This provided a strong signal for the involvement of the azomethine group (-CH=N) in chelation with the metal ion [33]. The (C=N) thiazole ring of the free ligand at (1597 cm^{-1}), which was moved to lower

wave numbers upon coordination, provided a solid signal for the involvement of the (C=N) thiazole ring in chelation with the metal ion. This was shown by the fact that the ring was shifted to lower wave numbers after coordination.

The hydroxyl group, which showed up at a wavelength of around 3370 cm^{-1} in the case of the 8-hydroxy quinolone that served as the co-ligand for the HQ in Table 1, vanished when it was complexed with metal ions. These results demonstrate that the phenolic (-OH) group of the HQ ligand does, in fact, participate in the coordination of metal ions after deprotonation. After coordination with the metal ion, the (C=N) of the quinoline moiety, which had first been seen at a wave number of 1588 cm^{-1} while the HQ co-ligand was bare, moved to a lower wave number. This shift provided proof that the (C=N) group of the co-ligand was involved in the chelation reaction with the metal ion.

The appearance of a wide band in the complexes with a frequency greater than 3400 cm^{-1} has been attributed to the -OH group of water molecules. In the spectra of the complexes, in the ranges 524-533 and 438-445, new bands have been discovered. These new bands have been given the numbers (M-O) and (M-N) [34], respectively, as shown in Table 1.

Magnetic measurement and electronic spectra

As indicated in the supplementary data, Table 1, the UV-Vis spectra of the created compounds illustrate that the characteristic ligand peak bathochrometically changes, and in addition, new peaks arise in the metal complexes. This can be seen in the spectra of the produced compounds. This exhibited the fact that there are complexes involving ligands and metal ions. The effective magnetic moment, also known as $\mu_{eff} = 2.83$ $(((Mwt \times Xg)-(dia\ magnetic\ correction*T))^{1/2}$, is one of the most successful ways for exposing the structural geometry of the complexes [35].

The UV-Vis spectra indicate that the FeLQ complex has bands that are detectable at a wavelength of 385 nm. It is possible that the $^6A_{1g} \rightarrow T_{2g}(G)$ transitions that take place in the distorted octahedral geometry are responsible for this band. The μ_{eff} of the FeLQ complex is measured to be 5.94 B.M. when it is measured at the temperature of the surrounding air. This number, which would be ascribed to the d5 high spin ($t_{2g}^3\ e_g^2$) electron configuration, shows that the FeLQ complex exhibits an octahedral shape, which can be found in Table 1.

At a wavelength of 475.0 nm, there was seen to be a peak in the electronic spectrum that belonged to the CoLQ complex. The transition of $^4T_{1g}(F) \rightarrow {}^4T^{2g}(F)$, which is suggestive of an octahedral structure, may be responsible for this peak's appearance. 4.85 B.M. is the temperature at which it is expected that the value of the CoLQ complex's μ_{eff} will be while it is at 25 °C. This number, which may be ascribed to the d7 high spin ($t_{2g}^5\ e_g^2$) electron configuration, shows that the CoLQ compound has an octahedral structure, which can be found in Table 1.

There are bands centered around 540.0 nm that may be seen in the electronic spectra of the NiLQ complex. As can be seen in Table 1, these bands may be explained by the $^3T_1(F) \rightarrow {}^3T_1(P)$ transitions, which point to an octahedral geometry around the Ni(II) core. The estimated value of the NiLQ compound's μ_{eff}, which is 3.17 B.M. and has the electron configuration corresponding to d8 ($(t_{2g}^6\ e_g^2)$), indicates that the octahedral geometry is present in the molecule. Table 1 displays these values.

A spectral band that centers at 550 nm may be seen in the electronic spectra of the CuLQ complex. There is a possibility that these bands are linked to the $^2B_{1g} \rightarrow {}^2A_{1g}$ transitions, which point to an octahedral geometry centered on the copper(II) core. This information can be found in Table 1. According to Table 1, the backbone-to-d^9 ($t_{2g}^6\ e_g^3$) electron configuration of the CuLQ compound has an estimated value of 1.93 B.M. for its effective electron configuration, which implies an octahedral shape. The LMCT is in charge of the band in the electronic spectra of the ZnL complex that may be found at a wavelength of 400 nm. There is some speculation that the octahedral geometry of the ZnLQ complex, which can be found in Table 1, is responsible for the diamagnetic feature of the ZnLQ complex.

Stoichiometry of the prepared complexes

The stoichiometry of the synthesized metal complexes that were generated in solution as a consequence of the interaction of the metal ion with the examined ligands was measured by using the spectrophotometric molar ratio technique [36]. This reaction occurred as a result of the metal ion reacting with the ligands. The creation of the complex is shown to occur at a molar ratio of 1:1:1 (M:L:Q) in the graph of the molar ratio plot, which consists of two linear parts crossing at a molar ratio of less than one.

Thermal analysis of the investigated mixed-ligand complexes

After subjecting the metal complexes to thermal analysis (both TGA and DTA), the researchers were able to get more accurate estimations of the structures of the metal complexes [37]. Counting the amount of water molecules that were either coordinated or uncoordinated was the method that was used to achieve this goal.

The synthesized complexes showed three degradation steps, Figure 1. The first degradation step led to founding (calc.) a weight loss percentage of 35.68 (35.58), 29.65 (29.69), 39.42 (39.36), 30.59 (30.59), and 35.11 (34.95)%, suggested the elimination of ($C_8H_{11}N_2O_2ClS$), (H_2O+$C_7H_8NO_2Cl$), (H_2O+$C_8H_{12}N_2O_2ClS$), (H_2O+C_9H_7NOCl) and (H_2O+$C_{10}H_{10}N_2OCl$) molecules for FeLQ, CoLQ, NiLQ, CuLQ, and ZnLQ, respectively. The thermal decomposition continued for the second and third decomposition steps leading to the removal of the residual organic moiety leaving the metal as a metallic deposit, Figure 1.

Mass spectra

The following molecular structures have been hypothesized to exist in metal complexes: [Fe(L)(Q)$(Cl)_2$], [Co(L)(Q)(H_2O)(Cl)], [Cu(L)(Q)(H_2O)(Cl)], [Ni(L)(Q)(H_2O)(Cl)], and [Zn(L)(Q)(H_2O)(Cl)]. The finding was made by comparing the masses of the molecules' chemical formulas to the mass spectra (m/z) readings of the molecules, which led to the discovery. The molecular ion peak, designated by the symbol M^+, was seen in the mass spectra of the compounds FeLQ, CoLQ, NiLQ, and CuLQ, respectively. These peaks were located at m/z values of 660.054, 644.982, 645.084, and 651.084 g/mol. This is an outstanding covenant when the complexes' formula weights, which are as follows: 660.35, 645.99, 645.76, 650.61, and 652.47, are considered. In addition to the formula that was suggested, it is important to emphasize the fact that the results of the mass spectra are in very good agreement with the results that were obtained for carbon, hydrogen, and nitrogen. This is a point that has to be emphasized.

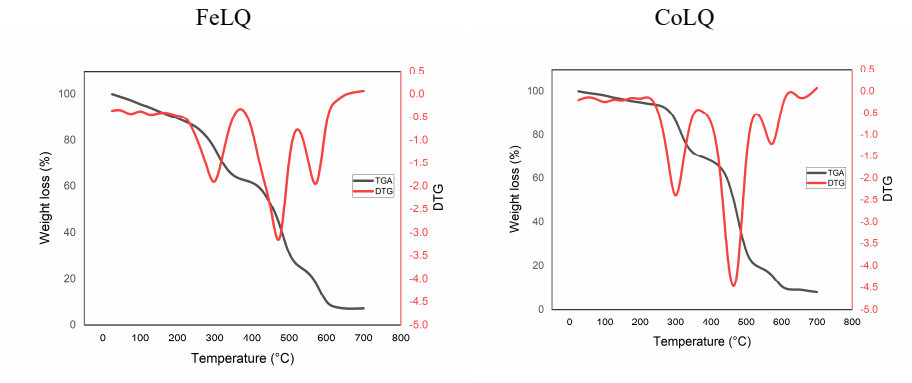

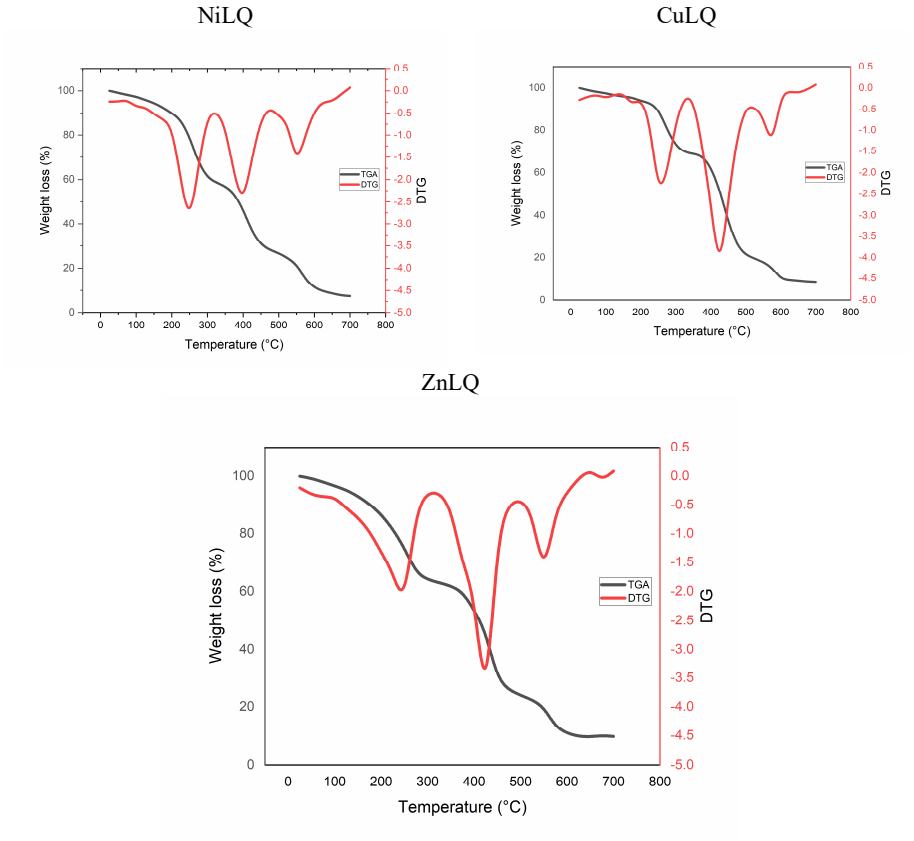

Figure 1. Thermal decomposition of the prepared FeLQ, CoLQ, NiLQ, CuLQ, and ZnLQ compounds at temperatures ranging from 25 degrees Celsius to 600 ºC.

Deduction of complex construction

The accumulation of all of the earlier findings suggests that the Schiff base ligand (L) participates as a neutral bi-dentate ligand through the Nitrogen thiazole and azomethine group, whereas the 8-hydroxy quinoline co-ligand (HQ) participates as a mono-negatively bi-dentate via the phenolic -OH, and –C=N, to form M:L:Q (1:1:1) as the overall molecular formula; $[Fe(L)(Q)(Cl)_2]$, $[Co(L)(Q)(H_2O)(Cl)]$, $[Cu(L)(Q)(H_2O)(Cl)]$, $[Ni(L)(Q)(H_2O)(Cl)]$, and $[Zn(L)(Q)]$ for the FeLQ, CoLQ, NiLQ, CuLQ, and ZnLQ, compounds, respectively, Scheme 1.

Modeling 3D structures

Because of a lack of data obtained via X-ray crystallography, the use of molecular modelling as a method that may be used to investigate the structural components that make up coordination compounds has become more significant. The reason for this is that molecular modelling not only offers the conformation of the molecule that has the lowest energy but also adds structural information about the molecule.

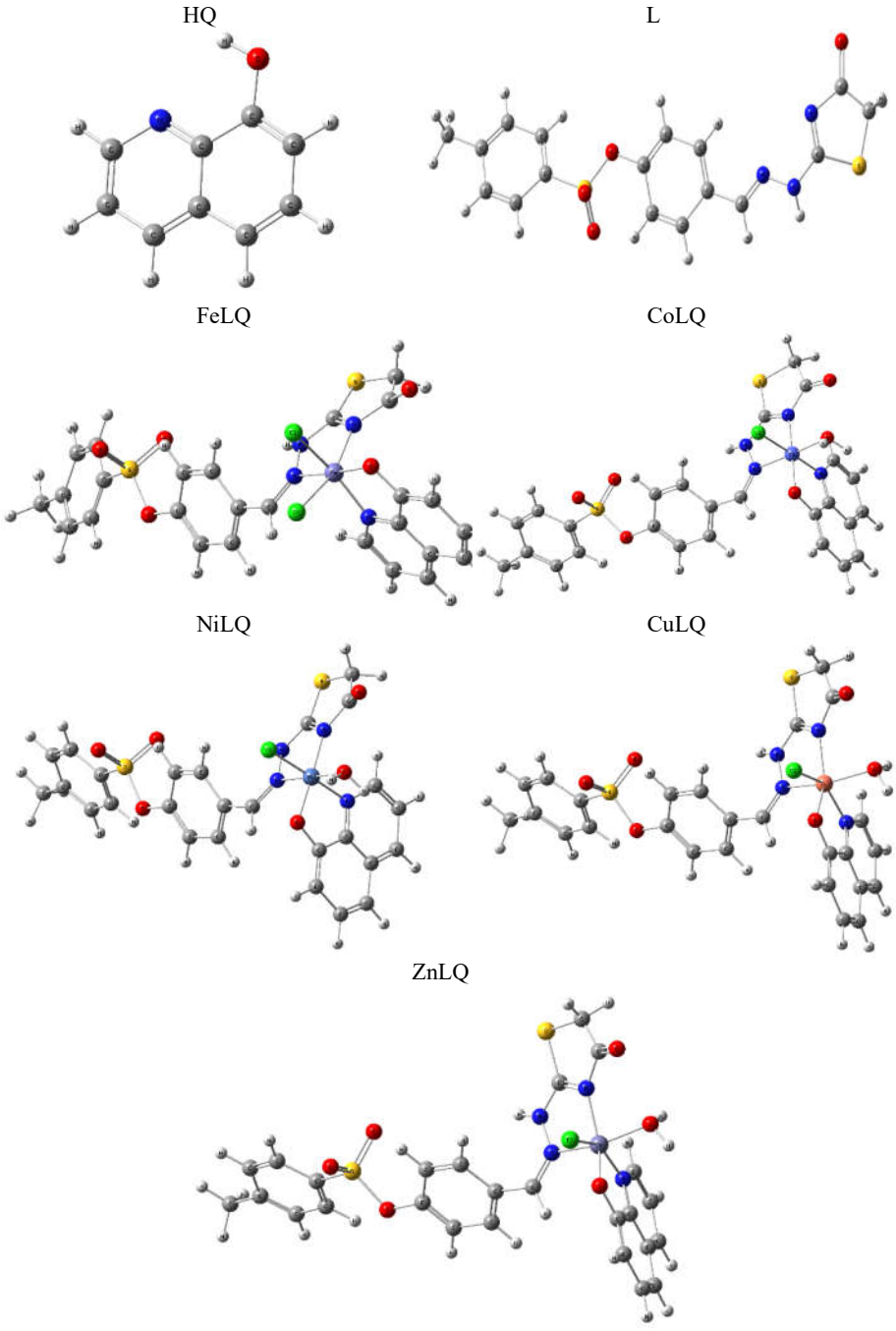

Figure 2. 3D configuration of the prepared ligands and their complexes.

Optimization of FeLQ, CoLQ, NiLQ, CuLQ, and ZnLQ compounds provided octahedral shape around the Fe(III), Co(II), Ni(II), Cu(II), and Zn(II) center, as; $[Fe(L)(Q)(Cl)_2]$, $[Co(L)(Q)(H_2O)(Cl)]$, $[Ni(L)(Q)(H_2O)(Cl)]$, $[Cu(L)(Q)(H_2O)(Cl)]$, and $[Zn(L)(Q)(H_2O)(Cl)]$, respectively, Figure 2.

It is very necessary to have a grasp of a molecule's frontier molecular orbitals (FMO), lowest unoccupied molecular orbital (LUMO), and highest occupied molecular orbital (HOMO) in order to have an appreciation for the molecule's reactivity, chemical stability, optical, and electrical properties [38]. Figure 3 illustrates the HOMO and LUMO configurations of the atomic orbitals of the complexes that we have been discussing up to this point. These configurations are shown in the atomic orbitals of the complexes. As a direct result of this, the vast majority of the molecule's electrons are scattered throughout a variety of the various locations.

Researchers are able to evaluate a molecule's chemical reactivity, kinetic stability, biological activity, hardness-softness, and polarizability when they analyze HOMO-LUMO energies. This is one of the reasons why this area of study is regarded to be so exciting. Another reason why this field of study is thought to be so intriguing is because it allows researchers to investigate the polarizability of molecules. Because the HOMO was the electron-containing orbital that was located the furthest from the nucleus, it was also the orbital that lost the greatest number of electrons. In addition to its function as an electron acceptor, the low-lying unoccupied mode of orbital, also known as LUMO, had the distinction of being the empty orbital that was situated in the region that was in immediate proximity to the nucleus. Consequently, the HOMO and LUMO orbitals of a molecule determine a molecule's reactivity with electrophiles and nucleophiles, respectively. The magnitude of the free energy difference, or E, may provide some insight into the reactivity of the molecules. Because E is the smaller of the two molecules, it is the one that responds more strongly to docking. According to this, the complex with the greatest degree of reactivity is the ZnLQ, followed by the CuLQ, then the NiLQ, then the FeLQ, then the CoLQ, then the HQ, and finally the L.

In addition to a compound's chemical reactivity, the degree to which it may be hard or soft is one of the most critical criteria that goes into determining its position in the ranking system. It is possible to describe the tendency of one molecule to interact with another molecule by using a rule that is often known as the hard-soft-acid-base rule, or the HSAB rule. In accordance with this rule, hard acids prefer to link with hard bases, while soft acids like making connections with soft bases [39]. The cell, proteins, and other fundamental constituents of living things are all examples of soft biological molecules. Because of this, the possibility of interaction between soft molecules and biological molecules is much higher for soft molecules than it is for hard molecules. Because of this, the presence of softness stimulates biological activity, while the presence of hardness suppresses it. As a consequence of this, the order in which reactions take place should be as follows; the items are listed in decreasing order of frequency, from the fewest to the most abundant: According to Table 2, ZnLQ performs better than CuLQ, NiLQ, FeLQ, CoLQ, and HQ.

Table 2. The calculated DFT parameters of the titled ligands and corresponding complexes.

	E_{HOMO}	E_{LUMO}	ΔE	I	A	χ		η	σ	ω	Nu	ΔN_{max}
HQ	-6.02	-1.77	4.25	6.02	1.77	3.89	-3.89	2.12	0.24	3.57	0.28	1.83
L	-6.62	-2.45	4.17	6.62	2.45	4.53	-4.53	2.09	0.24	4.92	0.20	2.17
FeLQ	-4.29	-3.16	1.12	4.29	3.16	3.72	-3.72	0.56	0.89	12.33	0.08	6.62
CoLQ	-4.94	-2.43	2.51	4.94	2.43	3.69	-3.69	1.26	0.40	5.41	0.18	2.94
NiLQ	-3.42	-2.43	0.99	3.42	2.43	2.93	-2.93	0.50	1.01	8.65	0.12	5.91
CuLQ	-3.62	-2.64	0.98	3.62	2.64	3.13	-3.13	0.49	1.02	9.96	0.10	6.37
ZnLQ	-3.18	-2.54	0.64	3.18	2.54	2.86	-2.86	0.32	1.56	12.79	0.08	8.94

The observation that the chemical potential for the studied complexes had a negative value indicated that the complexes have a high degree of stability [40]. It is more likely for the substance

to behave electrophilically owing to the fact that its electrophilicity index is high while its chemical potential value is low [41]. This is because the electrophilicity index is inversely proportional to the chemical potential value.

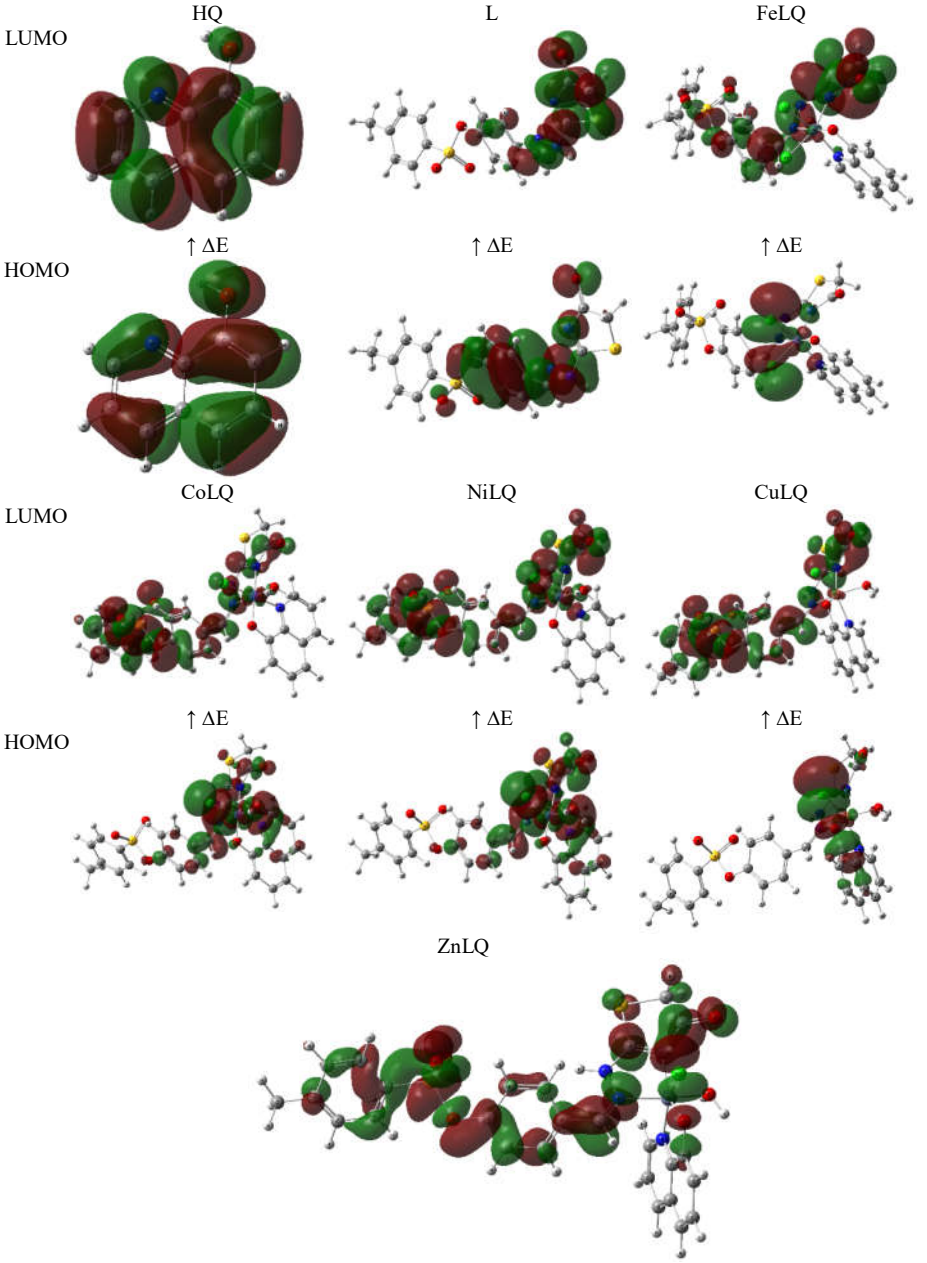

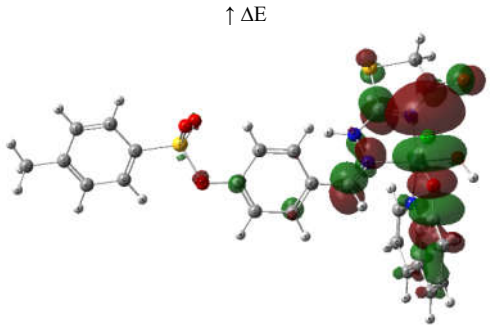

Figure 3. HOMO-LUMO constructions of the subject ligands and consistent complexes.

Both the substrate and the protein have partial charges, and these charges play a significant role in determining how well the substrate and the protein will bind to one another. It is possible to get information about the topological and structural features of substrates that exist in three dimensions by using a molecular electrostatic potential, or MEP, diagram [42]. The molecular electrostatic potential, abbreviated as MEP, is the property of a molecule that determines where in its geometry the nuclei or electrons exert the most amount of effect [43].

In order to provide a visual indication of the range of values that are shown in the diagram, an MEP diagram will employ a gradient of colours that goes from blue to red. There is a link between the electrophilic (blue) and nucleophilic (red) regions of the MEP, which are responsible for electrophilic and nucleophilic reactivity, respectively. The positively charged region is denoted by the colour blue. The presence of a negative charge on the surface is reflected by the red colours; specifically, those portions of the surface that have the greatest potential to receive an electrophile [44]. When the negative charge of a molecule grows, it is a sign that the important sites on that compound are becoming more attracted to electrophiles as processes occur. This happens when a molecule's charge becomes more negative.

In the substrates of interest, the bulk of the negative sites, denoted by red, can be observed clustered around the 8-hydroxy quinoline oxygen moiety. This is illustrated by the color red. Because this oxygen moiety is itself encircled by a significant number of electrons, it is an alluring target for electrophilic assault. The more positive regions, shown by blue, are mostly oriented towards the coordinated H_2O moiety, which has the potential to operate as an H-bond donor in protein-substrate intermolecular interactions.

Antimicrobial in vitro screening

In comparison to the antibacterial activity of the free ligands, the antibacterial activity of the newly developed compounds including FeLQ, CoLQ, NiLQ, CuLQ, and ZnLQ was dramatically increased. When we take into account the chelation principle [45], we are able to understand why the compounds FeLQ, CoLQ, NiLQ, CuZnLQ, and ZnLQ shown in Table 3 and Figure 4 have a lower level of activity in comparison to their respective pure ligands. According to this idea, the polarity of metal ions may be rendered less severe by the process of chelation. This is accomplished by partly sharing the positive charge of the metal ion with donor groups and through the potential delocalization of electrons over the whole of the ring. The lipophilicity of the complex is raised as a result of this, which makes it more likely that it will permeate the lipid bilayer that makes up the cell membrane. It is possible that the complex will have an influence on the metabolic pathways as well as the respiration process. This is because the complex will interfere with the binding sites of the microorganisms. Because of this, the production of proteins

is rendered impossible, which stymies the growth of the organism and, in the end, leads to the demise of the germs.

In addition, the activity index of the discovered compounds varied from 35.00% to 55.00% for the free ligands, and it rose to be in the range of 66.00% to 94.44% for the metal complexes, as indicated in Table 3 and Figure 4.

Molecular docking

During this investigation, the antimicrobial target protein was docked with the chemicals that were created. This was done in order to confirm the relationship between the in vitro anti-microbial outcomes and the binding attractions of the inhibitors. In other words, we wanted to see whether there was a correlation between the two. Molecular docking studies make it feasible to generate predictions about which compounds have the highest binding affinities by using virtual compound screening and scoring procedures [46, 47]. These approaches make it possible to determine which molecules have the potential to form the most stable bonds. The active site binding of a target receptor and a substrate is an example of an interaction that can be analyzed using this method, which interprets the interaction between two molecules as if they were parts of a three-dimensional jigsaw puzzle and then analyzes the findings according to this model [48, 49].

For the sake of this investigation, the materials that were created stand in for the substrate, and the protein from *E. coli* that has the identification number 1FJ4 in the protein data bank acts as the receptor. The outcomes of the molecular docking are shown in Table 4, and Figure 5 depicts how the best conformation of the studied substrates should be positioned inside the binding pocket.

Unbelievably, as can be seen in Figure 5 and Table 4, the listed substrates form connections with the *E. coli* (the structure of beta-ketoacyl-[acyl carrier protein] synthase i in complex with thiolactomycin, implications for drug design, PDB ID: 1FJ4) pocket through hydrophobic attractions with significant negative docking scores (S) and a large number of hydrogen bonds. This notion receives support from the tight coordination that takes place between docked substrates and the active area of the receptor. The rankings are as follows, with ZnLQ coming in first, followed by CoLQ, then NiLG, then FeLG, then CuLG, and finally L, in ascending order of inhibitory activity. Compound ZnLQ is the most active and forms a strong link to the substrate binding pocket of *E. coli* (the structure of beta-ketoacyl-[acyl carrier protein] synthase i in complex with thiolactomycin, implications for drug design, PDB ID: 1FJ4) by forming a variety of hydrogen bond contacts with GLY 205, ASP 227, THR 302, and GLY 305. These results can be found in Figure 5 and Table 4. Because of this, the compound ZnLG is the most promising contender for future investigation.

Table 3. Antimicrobial activity data.

		HQ	L	FeLQ	CoLQ	NiLQ	CuLQ	ZnLQ
P. aeruginosa (-ve)	IZ	8	9	14	17	16	19	19
	%	38.10	47.62	66.67	80.95	76.19	90.48	90.48
E. coli (–ve)	IZ	7	8	14	16	13	17	18
	%	35.00	45.00	70.00	80.00	65.00	85.00	90.00
S. aureus (+ve)	IZ	8	9	14	17	14	17	18
	%	42.11	47.37	73.68	89.47	73.68	89.47	94.74
B. cereus (+ve)	IZ	7	7	16	16	17	17	17
	%	35.00	40.00	80.00	80.00	85.00	85.00	85.00
A. flavus	IZ	7	8	17	18	17	18	18
	%	38.89	44.44	94.44	100.00	94.44	100.00	100.00
T. rubrum	IZ	8	8	16	17	16	17	17
	%	42.11	47.37	84.21	89.47	84.21	89.47	89.47
C. albicans	IZ	8	9	16	17	16	17	17
	%	44.44	55.56	88.89	94.44	88.89	94.44	94.44

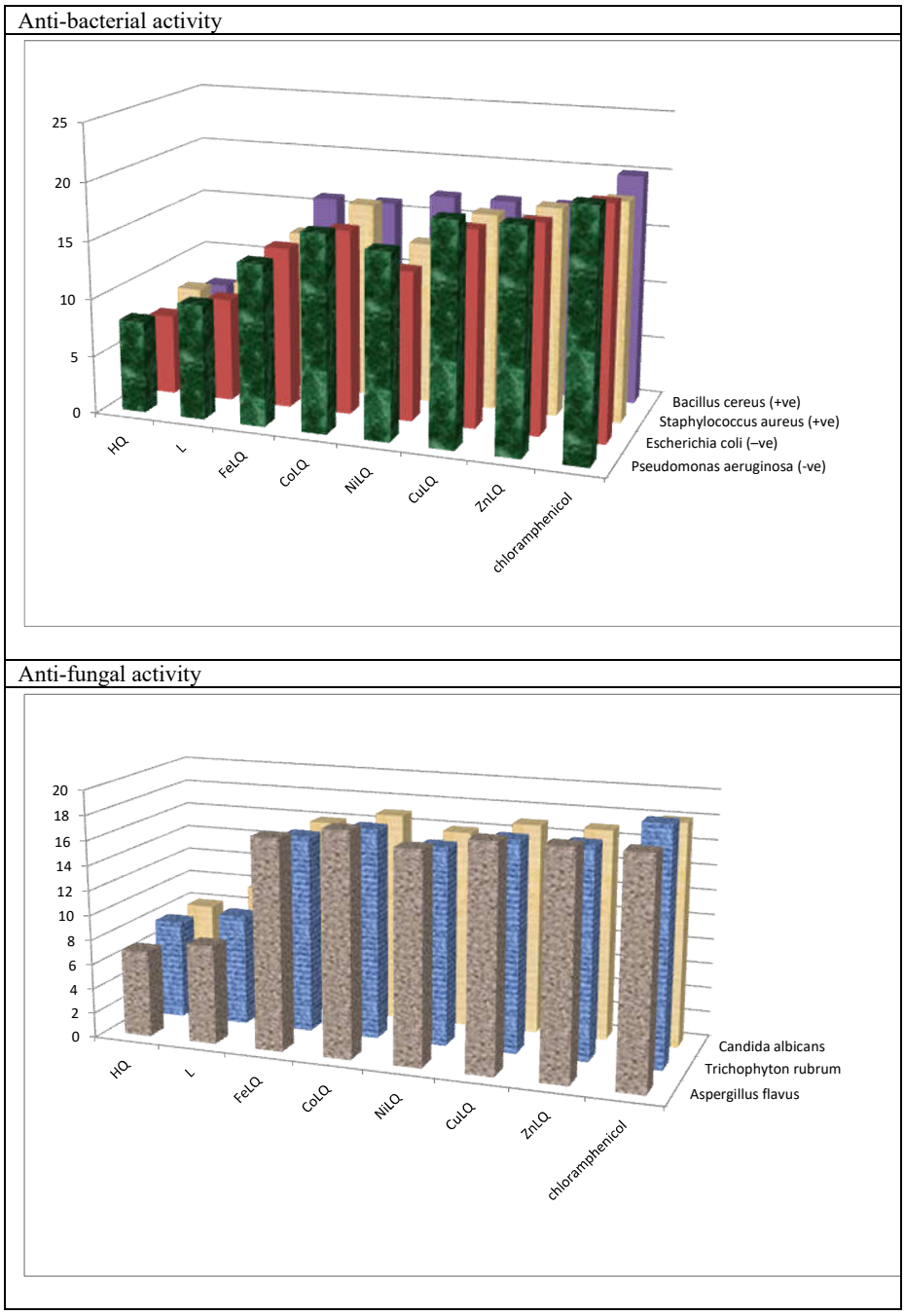

Figure 4. Antimicrobial activity data of the prepared FeLQ, CoLQ, NiLQ, CuLQ, and ZnLQ compounds using the disc diffusion method.

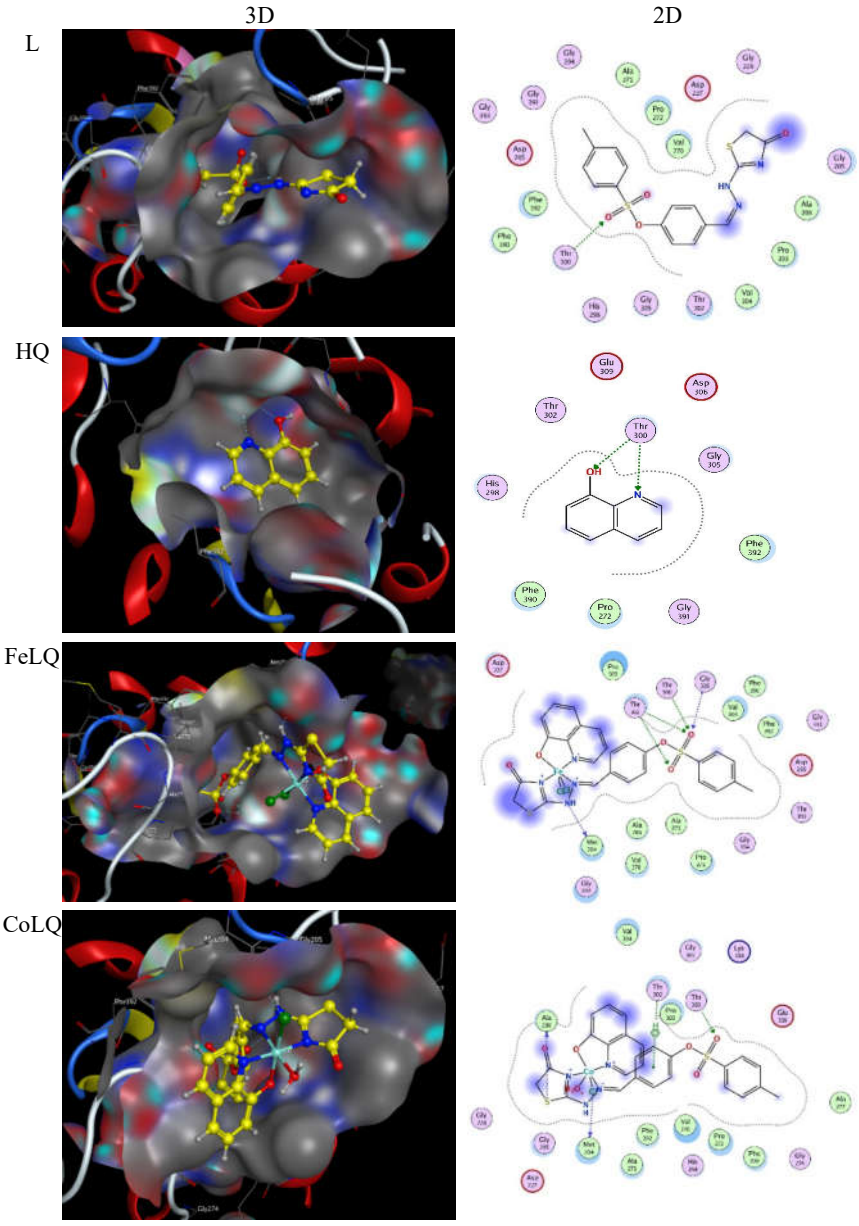
3D
2D
L
HQ
FeLQ
CoLQ

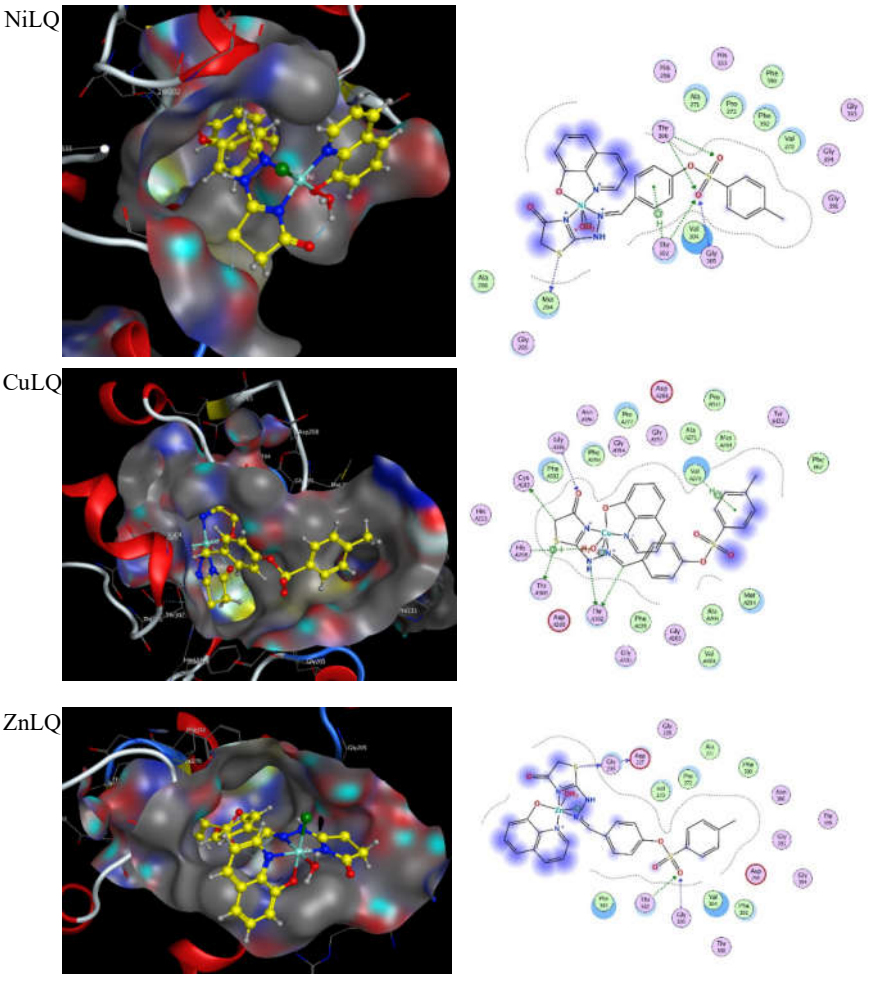

Figure 5. 3D, and 2D orientation of the substrate-protein complex.

Table 4. Molecular docking findings of the prepared materials.

	Ligand	Receptor	Interaction	Distance (Å)	E (kcal/mol)	S (kcal/mol)
HQ	N 3	THR 300	H-acceptor	3.16	-2.30	-5.77
	O 11	THR 300	H-acceptor	2.96	-0.90	
L	O 9	THR 300	H-acceptor	3.25	-1.30	-7.75
FeLQ	N 3	MET 204	H-donor	3.03	-2.00	-8.67
	O 24	THR 302	H-acceptor	3.32	-0.70	
	O 25	THR 300	H-acceptor	3.02	-1.40	
	O 25	THR 302	H-acceptor	3.06	-1.70	
	O 25	GLY 305	H-acceptor	3.64	-0.80	
CoLQ	S 5	ALA 206	H-donor	3.72	-0.40	-9.24
	CL 14	MET 204	H-donor	3.01	-0.50	
	O 24	THR 300	H-acceptor	2.99	-1.80	

	6-ring	THR 302	pi-H	3.89	-1.20	
NiLQ	S 5	MET 204	H-donor	3.14	-1.00	-9.07
	O 24	THR 300	H-acceptor	2.82	-2.00	
	O 24	THR 302	H-acceptor	3.43	-0.70	
	O 24	GLY 305	H-acceptor	3.46	-1.10	
	O 25	THR 300	H-acceptor	3.20	-1.20	
	6-ring	THR 302	pi-H	3.75	-0.60	
CuLQ	C 1	THR 302	H-donor	3.32	-1.10	-8.55
	N 3	THR 302	H-donor	3.19	-5.50	
	S 5	THR 300	H-donor	3.54	-0.70	
	C 7	CYS 163	H-donor	3.66	-0.80	
	O 9	GLY 391	H-acceptor	3.70	-0.70	
	O 15	HIS 298	cation-pi	4.55	-0.80	
	6-ring	VAL 270	pi-H	3.70	-1.00	
ZnLQ	S 5	GLY 205	H-donor	3.25	-0.62	-9.13
	S 5	ASP 227	H-donor	3.77	-0.40	
	O 24	THR 302	H-acceptor	3.02	-1.50	
	O 24	GLY 305	H-acceptor	3.15	-0.70	

CONCLUSION

The structures of five synthesized FeLQ, CoLQ, NiLQ, and ZnLQ complexes were investigated. According to the findings, the L and Q ligands play the role of a neutral and monobasic bi-dentate NN or ON ligand, and they coordinate to the metal ions in a molar ratio of 1:1:1 for M:L:Q. The magnetic and electronic spectrum measurements indicated that the title complexes could have a deformed octahedral geometry. Calculations using DFT were used to examine potential structural improvements and Optimizations. According to the molecular electrostatic potential (MEP), it was discovered that the atoms of nitrogen and oxygen in the ligands that were being investigated had the greatest potential for electrostatic repulsion. Pathogenic bacterial and fungal strains that are often discovered as contaminants in the Arab environment were used for *in vitro* examinations of the antibacterial and antifungal properties of free ligands and their metal complexes. According to the data, the antibacterial and antifungal candidate activity of metal complexes is much higher than that of their free ligands. In addition, the outcome of molecular docking experiments showed the binding free energy of the title complexes with the active sites of the receptor of gram-negative bacteria: *E. coli* (PDB ID: 1FJ4). These studies also demonstrated that for the examined complexes, the stronger the contact, the more negative the binding energy. The ZnLQ complex showed the greatest binding of these medicines to their respective receptors than any other complex.

ACKNOWLEDGMENTS

The authors acknowledge the Deanship of Scientific Research, Vice Presidency for Graduate Studies and Scientific Research at King Faisal University, Saudi Arabia, for financial support under the annual funding track (GRANT 1779).

REFERENCES

1. El-Sonbati, A.; El-Mogazy, M.; Nozha, S.; Diab, M.; Abou-Dobara, M.; Eldesoky, A.; Morgan, S.M. Mixed ligand transition metal(II) complexes: Characterization, spectral, electrochemical studies, molecular docking and bacteriological application. *J. Mol. Struct.* **2022**, 1248, 131498.
2. Khan, H.Y.; Parveen, S.; Yousuf, I.; Tabassum, S.; Arjmand, F. Metal complexes of NSAIDs as potent anti-tumor chemotherapeutics: Mechanistic insights into cytotoxic activity via multiple pathways primarily by inhibition of COX–1 and COX–2 enzymes. *Coord. Chem. Rev.* **2022**, 453, 214316.

3. Dar, O.A.; Lone, S.A.; Malik, M.A.; Aqlan, F.M.; Wani, M.Y.; Hashmi, A.A. Ahmad, A. Synthesis and synergistic studies of isatin based mixed ligand complexes as potential antifungal therapeutic agents. *Heliyon* **2019**, 5, e02055.
4. Gull, P.; Dar, O.A.; Malik, M.A.; Hashmi, A.A. Design, synthesis, characterization and antimicrobial/antioxidant activities of 1,4-dicarbonyl-phenyl-dihydrazide based macrocyclic ligand and its Cu(II), Co(II) and Ni(II) complexes. *Microb. Pathog*. **2016**, 100, 237-243.
5. Malik, M.A.; Raza, M.K.; Dar, O.A.; Abid, M.; Wani, M.Y.; Al-Bogami, A.S.; Hashmi, A.A. Probing the antibacterial and anticancer potential of tryptamine based mixed ligand Schiff base ruthenium(III) complexes. *Bioorg. Chem.* **2019**, 87, 773-782.
6. Ayipo, Y.O.; Osunniran, W.A.; Babamale, H.F.; Ayinde, M.O.; Mordi, M.N. Metalloenzyme mimicry and modulation strategies to conquer antimicrobial resistance: Metal-ligand coordination perspectives. *Coord. Chem. Rev*. **2022**, 453, 214317.
7. Li, G.; Liu, H.; Feng, R.; Kang, T.-S.; Wang, W.; Ko, C.-N.; Wong, C.-Y.; Ye, M.; Ma, D.-L.; Wan, J.-B. A bioactive ligand-conjugated iridium (III) metal-based complex as a Keap1–Nrf2 protein-protein interaction inhibitor against acetaminophen-induced acute liver injury. *Redox Biol.* **2021**, 48, 102129.
8. Abd El-Lateef, H.M.; Khalaf, M.M.; El-Taib Heakal, F.; Abdou, A. Fe(III), Ni(II), and Cu(II)-moxifloxacin-tri-substituted imidazole mixed ligand complexes: Synthesis, structural, DFT, biological, and protein-binding analysis. *Inorg. Chem. Commun.* **2023**, 158, 111486.
9. Abd El-Lateef, H.M.; Khalaf, M.M.; Kandeel, M.; Abdou, A. Synthesis, characterization, DFT, biological and molecular docking of mixed ligand complexes of Ni(II), Co(II), and Cu(II) based on ciprofloxacin and 2-(1H-benzimidazol-2-yl) phenol. *Inorg. Chem. Commun*. **2023**, 155, 111087.
10. Khalil, E.A.; Mohamed, G.G. Synthesis and characterization of some transition and inner transition mixed ligand complexes derived from Schiff base ligand and *o*-aminophenol. *Inorg. Chem. Commun.* **2023**, 153, 110825.
11. Paison, F.; Su, B.; Pan, D.; Yan, T.; Wu, J. The study of biological activities of various mixed ligand complexes of nickel(II). *Austin Biochem*. **2020**, 5, 1025.
12. Soltani, B.; Ghorbanpour, M.; Ziegler, C.J.; Ebadi-Nahari, M.; Mohammad-Rezaei, R. Nickel(II) and cobalt(II) complexes with bidentate nitrogen-sulfur donor pyrazole derivative ligands: Syntheses, characterization, X-ray structure, electrochemical studies, and antibacterial activity. *Polyhedron* **2020**, 180, 114423.
13. Crim, J.A.; Petering, H.G. The antitumor activity of Cu(II) KTS, the copper(II) chelate of 3-ethoxy-2-oxobutyraldehyde bis (thiosemicarbazone). *Cancer Research* **1967**, 27, 1278-1285.
14. Zafar, W.; Ashfaq, M.; Sumrra, S.H. A review on the antimicrobial assessment of triazole-azomethine functionalized frameworks incorporating transition metals. *J. Mol. Struct.* **2023**, 1288, 135744.
15. Saadeh, H.A.; Sweidan, K.A.; Mubarak, M.S. Recent advances in the synthesis and biological activity of 8-hydroxyquinolines. *Molecules* **2020**, 25, 4321.
16. Shoji, E.; Miyatake, K.; Hlil, A.; Hay, A.; Maindron, T.; Jousseaume, V.; Dodelet, J.; Tao, Y.; D'iorio, M. Immiscible polymers in double spin-coated electroluminescent devices containing phenyl-substituted tris (8-hydroxyquinoline) aluminum derivatives soluble in a host polymer. *J. Polym. Sci.* **2003**, 41, 3006-3016.
17. Abd El-Lateef, H.M.; Khalaf, M.M.; Gouda, M.; Kandeel, M.; Amer, A.A.; Abdelhamid, A.A.; Drar, A.M.; Gad, M.A. Functionalized pyridines: Synthesis and toxicity evaluation of potential insecticidal agents against *Aphis craccivora*. *ACS Omega* **2023**, 8, 29685-29692.
18. Abdelhamid, A.A.; Aref, S.A.; Ahmed, N.A.; Elsaghier, A.M.; Abd El Latif, F.M.; Al-Ghamdi, S.N.; Gad, M.A. Design, synthesis, and toxicological activities of novel insect growth regulators as insecticidal agents against *Spodoptera littoralis* (Boisd.). *ACS Omega* **2022**, 8, 709-717.
19. Ali, A.M.; Salah, H.; Gad, M.A.; Youssef, M.A.M.; Elkanzi, N.A. Design, synthesis, and SAR studies of some novel chalcone derivatives for potential insecticidal bioefficacy screening on *Spodoptera frugiperda* (Lepidoptera: Noctuidae). *ACS Omega* **2022**, 7, 40091-40097.

20. Bakry, M.; Mohammed, L.; Dabour, N.; Gad, M. Design and synthesis of novel N,N′-substituted benzamide derivatives as potential insecticidal agents against the white mango scale insect, *Aulacaspis tubercularis* (Hemiptera: Diaspididae). *Curr. Chem. Lett.* **2024**, 13, 173-186.
21. Elkanzi, N.A.; Al-Hazmi, A.K.G.; Bakr, R.B.; Gad, M.A.; Abd El-Lateef, H.M.; Ali, A.M. Design and synthesis of pyridine and thiazole derivatives as eco-friendly insecticidal to control olive pests. *Chem. Biodivers*. **2023**, 20, e202300559.
22. El-Saghier, A.M.; Abosella, L.; Aborahma, G.A.; Elakesh, E.O.; Abdelhamid, A.A.; Gad, M.A. Synthesis and insecticide evaluation of some new oxopropylthiourea compounds as insect growth regulators against the cotton leafworm, *Spodoptera littoralis*. *Sci. Rep.* **2023**, 13, 13089.
23. Gad, M.; Bakry, M.; Shehata, E.; Dabour, N. Insecticidal thioureas: Preparation and biochemical impacts of some novel thiobenzamide derivatives as potential eco-friendly insecticidal against the cotton leafworm, *Spodoptera littoralis* (Boisd.). *Curr. Chem. Lett.* **2023**, 12, 685-694.
24. Abd El-Lateef, H.M.; Khalaf, M.M.; Kandeel, M.; Amer, A.A.; Abdelhamid, A.A.; Abdou, A. New mixed-ligand thioether-quinoline complexes of nickel(II), cobalt(II), and copper(II): Synthesis, structural elucidation, density functional theory, antimicrobial activity, and molecular docking exploration. *Appl. Organomet. Chem*. **2023**, 37, e7134.
25. Jarad, A.J.; Dahi, M.A.; Al-Noor, T.H.; El-ajaily, M.M.; AL-Ayash, S.R.; Abdou, A. Synthesis, spectral studies, DFT, biological evaluation, molecular docking and dyeing performance of 1-(4-((2-amino-5-methoxy) diazenyl) phenyl) ethanone complexes with some metallic ions. *J. Mol. Struct.* **2023**, 1287, 135703.
26. Murugan, T.; Venkatesh, R.; Geetha, K.; Abdou, A. Synthesis, spectral investigation, DFT, antibacterial, antifungal and molecular docking studies of Ni(II), Zn(II), Cd(II) complexes of tetradentate Schiff-base ligand. *Asian J. Chem.* **2023**, 35, 1509-1517.
27. Balouiri, M.; Sadiki, M.; Ibnsouda, S.K. Methods for in vitro evaluating antimicrobial activity: A review. *J. Pharm. Anal*. **2016**, 6, 71-79.
28. Abd El-Lateef, H.M.; Khalaf, M.M.; Kandeel, M.; Amer, A.A.; Abdelhamid, A.A.; Abdou, A. Designing, characterization, biological, DFT, and molecular docking analysis for new FeAZD, NiAZD, and CuAZD complexes incorporating 1-(2-hydroxyphenylazo)-2-naphthol (H2AZD). *Comput. Biol. Chem*. **2023**, 105, 107908.
29. Elkanzi, N.A.; Ali, A.M.; Hrichi, H.; Abdou, A. New mononuclear Fe(III), Co(II), Ni(II), Cu(II), and Zn(II) complexes incorporating 4-{[(2 hydroxyphenyl) imino] methyl} phenyl-4-methylbenzenesulfonate (HL): Synthesis, characterization, theoretical, anti-inflammatory, and molecular docking investigation. *Appl. Organomet. Chem*. **2022**, 36, e6665.
30. Mohapatra, R.K.; Mahal, A.; Ansari, A.; Kumar, M.; Guru, J.P.; Sarangi, A.K.; Abdou, A.; Mishra, S.; Aljeldah, M.; AlShehail, B.M. Comparison of the binding energies of approved Mpox drugs and phytochemicals through molecular docking, molecular dynamics simulation, and ADMET studies: An in silico approach. *J. Biosaf. Biosecurity*. **2023**, 5, 118-132.
31. Ali, I.; Wani, W.A.; Saleem, K. Empirical formulae to molecular structures of metal complexes by molar conductance. *Synth. React. Inorg. Met.* **2013**, 43, 1162-1170.
32. Abu-Dief, A.M.; El-Khatib, R.M.; El-Dabea, T.; Abdou, A.; Aljohani, F.S.; Al-Farraj, E.S.; Barnawi, I.O.; Ali, M.A.E.A.A. Fabrication, structural elucidation of some new metal chelates based on N-(1H-Benzoimidazol-2-yl)-guanidine ligand: DNA interaction, pharmaceutical studies and molecular docking approach. *J. Mol. Liq.* **2023**, 386, 122353.
33. Singh, K.; Thakur, R. Synthesis, spectroscopic studies and biological perspectives of transition metal complexes of N/S donor Schiff base. *Eur. Chem. Bull*. **2016**, 5, 193-201.
34. Latif, M.; Ahmed, T.; Hossain, M.S.; Chaki, B.; Abdou, A.; Kudrat-E-Zahan, M. Synthesis, spectroscopic characterization, DFT calculations, antibacterial activity, and molecular docking analysis of Ni(II), Zn(II), Sb(III), and U(VI) metal complexes derived from a nitrogen-sulfur Schiff base. *Russ. J. Gen. Chem*. **2023**, 93, 389-397.

35. Bain, G.A.; Berry, J.F. Diamagnetic corrections and Pascal's constants. *J. Chem. Educ*. **2008**, 85, 532.
36. Ahmed, M.; Narayanaswamy, R. Studies of equilibria involving the binary and ternary complexes of aluminium with eriochrome cyanine R (ECR) and cetylpyridinium chloride (CP). *Pertanika J. Sci. Technol*. **2005**, 13, 43-60.
37. Ali, M.A.E.A.A.; Elhady, O.; Abdou, A.; Alhashmialameer, D.; Eskander, T.N.A.; Abu-Dief, A.M. Development of new 2-(benzothiazol-2-ylimino)-2, 3-dihydro-1H-imidazol-4-ol complexes as a robust catalysts for synthesis of thiazole 6-carbonitrile derivatives supported by DFT studies. *J. Mol. Struct*. **2023**, 1292, 136188.
38. Hrichi, H.; Elkanzi, N.A.; Ali, A.M.; Abdou, A. A novel colorimetric chemosensor based on 2-[(carbamothioylhydrazono) methyl] phenyl 4-methylbenzenesulfonate (CHMPMBS) for the detection of Cu(II) in aqueous medium. *Res. Chem. Intermed*. **2023**, 49, 2257-2276.
39. Abdou, A.; Omran, O.A.; Al-Fahemi, J.H.; Jassas, R.S.; Al-Rooqi, M.M.; Hussein, E.M.; Moussa, Z.; Ahmed, S.A. Lower rim thiacalixarenes derivatives incorporating multiple coordinating carbonyl groups: Synthesis, characterization, ion-responsive ability and DFT computational analysis. *J. Mol. Struct.* **2023**, 1293, 136264.
40. Al-Wabli, R.I.; Resmi, K.; Mary, Y.S.; Panicker, C.Y.; Attia, M.I.; El-Emam, A.A.; Van Alsenoy, C. Vibrational spectroscopic studies, Fukui functions, HOMO-LUMO, NLO, NBO analysis and molecular docking study of (E)-1-(1,3-benzodioxol-5-yl)-4,4-dimethylpent-1-en-3-one, a potential precursor to bioactive agents. *J. Mol. Struct*. **2016**, 1123, 375-383.
41. Chaudhary, A.P.; Bharti, S.K.; Kumar, S.; Ved, K.; Padam, K. Study of molecular structure, chemical reactivity and first hyperpolarizability of a newly synthesized N-(4-oxo-2-phenylquinazolin-3(4H)-yl)-1H-indole-2-carboxamide using spectral analysis. *J. Mol. Struct*. **2017**, 1148, 356-363.
42. El-Saghier, A.M.; Abdou, A.; Mohamed, M.A.; Abd El-Lateef, H.M.; Kadry, A.M. Novel 2-acetamido-2-ylidene-4-imidazole derivatives (El-Saghier Reaction): Green synthesis, biological assessment, and molecular docking. *ACS Omega* **2023**, 8, 30519-30531.
43. Shokr, E.K.; Kamel, M.S.; Abdel-Ghany, H.; Ali, M.A.E.A.A.; Abdou, A. Synthesis, characterization, and DFT study of linear and non-linear optical properties of some novel thieno [2,3-b] thiophene azo dye derivatives. *Mater. Chem. Phys*. **2022**, 290, 126646.
44. El-Remaily, M.A.E.A.A.A.; El-Dabea, T.; El-Khatib, R.M.; Abdou, El Hamd, M.A.; Abu-Dief, A.M. Efficiency and development of guanidine chelate catalysts for rapid and green synthesis of 7-amino-4,5-dihydro-tetrazolo[1,5-a]pyrimidine-6-carbonitrile derivatives supported by density functional theory (DFT) studies. *Appl. Organomet. Chem*. **2023**, 37, e7262.
45. Uddin, M.N.; Chowdhury, D.A.; Islam, M.T.; Hoque, F. Evaluation of biological activity of dioxouranium complexes of some Schiff base and dithiocarbamate ligands. *Orbital: Electron. J. Chem*. **2012**, 4, 235-244.
46. Shaaban, S.; Abdou, A.; Alhamzani, A.G.; Abou-Krisha, M.M.; Al-Qudah, M.A.; Alaasar, M.; Youssef, I.; Yousef, T.A. Synthesis and in silico investigation of organoselenium-clubbed Schiff bases as potential Mpro inhibitors for the SARS-CoV-2 replication. *Life* **2023**, 13, 912.
47. Najar, A.M.; Eswayah, A.; Moftah, M.B.; Ruwida Omar, M.K.; Bobtaina, E.; Najwa, M.; Elhisadi, T.A.; Tahani, A.; Tawati, S.M.; Khalifa, A.M.M.; Abdou, A.; DowAltome, A.E. Rigidity and flexibility of pyrazole, s-triazole, and v-triazole derivative of chloroquine as potential therapeutic against COVID-19. *J. Med. Chem. Sci.* **2023**, 6, 2056-2084.
48. Shaaban, S.; Al-Faiyz, Y.S.; Alsulaim, G.M.; Alaasar, M.; Amri, N.; Ba-Ghazal, H.; Al-Karmalawy, A.A.; Abdou, A. Synthesis of new organoselenium-based succinanilic and maleanilic derivatives and in silico studies as possible SARS-CoV-2 main protease inhibitors. *Inorganics* **2023**, 11, 321.
49. Abd El-Lateef, H.M.; Khalaf, M.M.; Amer, A.A.; Kandeel, M.; Abdelhamid, A.A.; Abdou, A. Synthesis, characterization, antimicrobial, density functional theory, and molecular docking studies of novel Mn(II), Fe(III), and Cr(III) complexes incorporating 4-(2-hydroxyphenyl azo)-1-naphthol (Az). *ACS Omega* **2023**, 8, 25877-25891.